Front. Optoelectron. 2016, 9(3): 436–449
DOI 10.1007/s12200-016-0629-9

REVIEW ARTICLE

Silicon-plus photonics

Daoxin DAI (✉)[1], Yanlong YIN[1], Longhai YU[1], Hao WU[1], Di LIANG[2], Zhechao WANG[3], Liu LIU[4]

1 Centre for Optical and Electromagnetic Research, State Key Laboratory for Modern Optical Instrumentation, Zhejiang University, Hangzhou 310058, China
2 System Research Lab, Hewlett Packard labs, Palo Alto, CA, USA
3 Center for Nano- and Biophotonics (NB-Photonics), Ghent University, Sint-Pietersnieuwstraat 41, Ghent 9000, Belgium
4 SCNU-ZJU Joint Research Center of Photonics, Centre for Optical and Electromagnetic Research, South China Academy of Advanced Optoelectronics, South China Normal University, Guangzhou 510006, China

Abstract Silicon photonics has become very popular because of their compatibility with mature CMOS technologies. However, pure silicon is still very difficult to be utilized to obtain various photonic functional devices for large-scale photonic integration due to intrinsic properties. Silicon-plus photonics, which pluses other materials to break the limitation of silicon, is playing a very important role currently and in the future. In this paper, we give a review and discussion on the progresses of silicon-plus photonics, including the structures, devices and applications.

Keywords silicon-plus, hybrid, plsamonic, photodetector, modulator, graphene, III-V

1 Introduction

In the past decade, silicon photonics has become very popular because of their compatibility with mature CMOS technology, and great progresses have been achieved [1,2]. However, it is still very difficult to realize various photonic functional devices for large-scale photonic integration by utilizing the material system of pure silicon due to the intrinsic properties of silicon material. An effective solution is to develop silicon-plus photonics by introducing other materials to overcome the disadvantages of silicon. People have already tried to put various materials on silicon, e.g., metals [3], III-V semiconductors [4,5], group four materials (like germanium (Ge) [6], graphene [7–10], etc.), polymer [11,12], magnetic-optical materials [13], liquid-crystals [14], etc. In this way, silicon-plus photonics becomes very powerful and useful for various applications of optical communications as well as optical sensing in the wavelength range from visible light to mid-infrared light.

First, metal is a kind of material used widely for silicon photonics. Regularly metal is used to make electrodes/micro-heaters for the propagation of electrical signals or the supply of electrical power, which is indispensable for thermal-tunable/switchable silicon photonic integrated devices and active silicon photonic devices (including lasers, modulators and photodetectors). The process for making metal strips on silicon is easy, including sputtering and lift-off processes. Another important application of metal for silicon photonics is that one can realize nanoplasmonic waveguides on silicon so that the diffraction limit can be broken and thus ultra-compact silicon photonic devices can be realized [3]. This importance of shrinking the device footprints has been realized for a long time because the small footprint is helpful for achieving ultra-high integration density, ultra-high speed as well as ultra-low power consumption. In recent years, the combination of metal and silicon photonics has generated silicon hybrid plasmonics which is a very attractive new platform for photonic integration. Usually the metal absorption is not favorable for silicon photonics while the metal absorption loss can be possibly compensated by introducing some gain medium. On the other hand, the light absorption of metal can be utilized to detect light power by measuring the resistance of the metal strip illuminated by incident light.

Second, semiconductor materials (e.g., III-V, Ge) have been also introduced for silicon-plus photonics so that one can realize lasers, amplifier, photodetecors, electro-optical modulators. Note that there is usually a large lattice mismatch between these semiconductor materials (III-V, Ge) and silicon, one usually needs some special fabrication processes. For the combination of III-V and silicon, the most popular two technologies are the molecular bonding

Received February 18, 2016; accepted May 25, 2016

E-mail: dxdai@zju.edu.cn

developed at University of California, Santa Barbara, and the adhesive bonding at Ghent University. In these ways, III-V/silicon lasers [4], modulators, and photodetectors [5] have been developed very successfully in the past decade. Meanwhile, people have also been making great efforts to directly grow different semiconductor materials on silicon by optimizing the processes. Fortunately, there are some great progresses reported recently. For Ge, big progress has been achieved for the process of the epitaxial growth on silicon in recent years [15–18], e.g., using a two-step Ge epitaxial deposition. With the techniques of high-quality Ge growth on silicon, many Ge-on-Si active devices have been demonstrated, including high-speed optical modulators [16], metal-semiconductor-metal (MSM) photodetectors [17], and PIN photodetectors [18]. Low defect-density growth of GaAs [19] and InP [20] using selective-area growth on pre-patterned (001)-Si has been also demonstrated. By leveraging this technology, recently millimeter-long InP waveguide was directly grown on silicon, with superior material quality [21]. More recently, graphene has attracted lots of attention as one of the most attractive material to be working with silicon photonics because of its unique optoelectronic properties [22–24]. With the hybrid platform of graphene-silicon, one can achieve compact optical modulators [7,25] and high-speed photodetectors [8–10]. The large nonlinearity coefficient of graphene also makes it very attractive for all-optical devices [26–28].

Polymer materials are also very attractive for silicon-plus photonics because the fabrication processes are easy and compatible with silicon photonics. Furthermore, polymer materials can be synthesized as designed to be nonlinear optical materials with high nonlinear optical coefficients (e.g., electrical-optical coefficients), which is useful for realizing all-optical devices, and electrical optical modulators [11,12]. Polymer materials are also useful to compensate the serious temperature dependence of silicon photonic devices by utilizing the negative thermo-optical effect [29]. It is even possible to have gain medium based on polymer doped with some gain materials [30]. Therefore, the silicon-plus photonics with polymer is becoming more and more attractive.

In this paper, we give a review and discussion on the progresses of silicon-plus photonics, including the structures, devices and applications.

2 Silicon-plus photonics

Table 1 shows a summary of the materials developed for silicon-plus photonics in the past decade. The possible functionality and the available wavelength-range of these materials are also included in Table 1. In the following parts, we give an introduction for silicon-plus photonics with these materials.

2.1 Silicon-plus photonics with metals

Metal has been used very widely for silicon photonics as electrodes/micro-heaters for the propagation of electrical signals or the supply of electrical power, which is indispensable for thermal-tunable/switchable silicon photonic integrated devices, and the active silicon photonic devices (including lasers, modulators and photodetectors). Figure 1 shows a thermal-optical switch with metal micro-heaters [31] and the array. The fabrication processes for making metal strips on silicon is easy, including the sputtering processes, and the lift-off processes.

Another important application for silicon photonics with metal is that one can realize nanoplasmonic waveguides [32–35], which breaks the diffraction limit and thus enables ultra-compact silicon photonic devices. In recent years, the combination of metal and silicon photonics generates silicon hybrid plasmonics [35] which is a very attractive new platform for photonic integration.

Table 1 Summary of materials used for silicon-plus photonics

silicon + X material		function	visible sensing	near-infrared commun.	mid-infrared sensing
metal		heater	√	√	√
		hybrid plasmonics	√	√	√
		photothermal detector			√
III-V		laser, amplifier, photodetectors, modulators		√	√ (~2 μm)
II-VI		laser, amplifier, photodetectors, modulators			√
IV	Ge/Sn	lasers		√	
	Ge	photodetectors, modulators			
	graphene	photodetectors, modulators		√	√
polymer	EO* polymer	modulator		√	
	strong nonlinear effect	all-optical		√	
	polymer with dopants	emission, amplifier	√	√	

Note: *EO, electro-optic

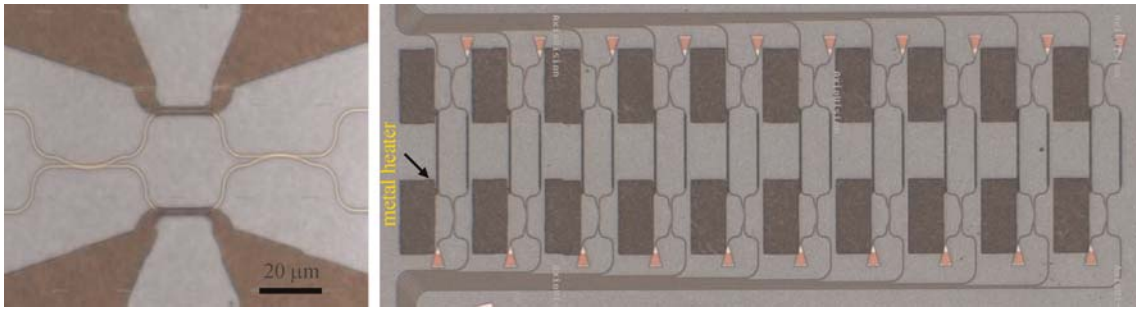

Fig. 1 Thermal-optical switch with metal micro-heaters and the array [31]

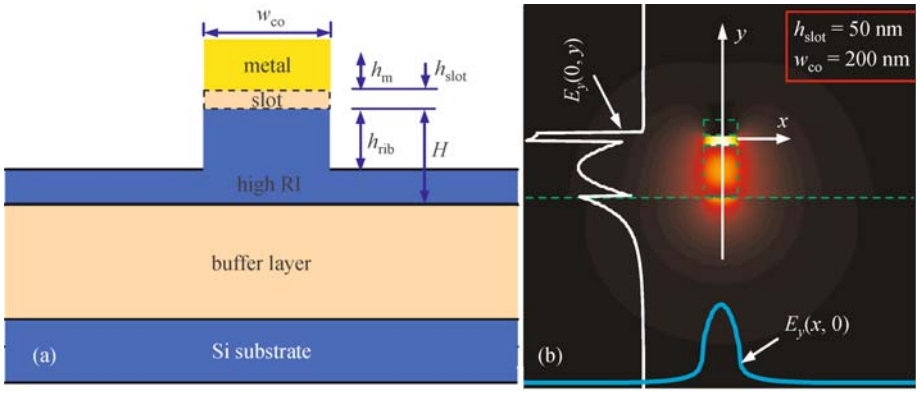

Fig. 2 Cross section of a silicon hybrid nanoplasmonic waveguide with a metal cap; (b) calculated field distribution for the quasi-TM fundamental mode when w_{co} = 200 nm and h_{slot} = 50 nm [35]

Figure 2(a) shows the cross section of a silicon hybrid nanoplasmonic waveguide, which consists of a silicon region, a metal layer and a low-index region between them. The low-index material could be SiO_2, Al_2O_3, SiN, or polymer when operating at near-infrared, which is the window for optical fiber communications. For the visible light range, which is useful for optical sensing, the high-index material could be Al_2O_3 or SiN, while the low-index material could be polymer, SiO_2, liquid, or gas. For the silicon hybrid plasmonic waveguides, the silicon core layer can be etched deeply or shallowly and the width of the metal strip does not have to be equal to that of the silicon core region. This makes the design of silicon hybrid plasmonic waveguides very flexible. As an example, when choosing $h_{Si\_rib} = h_{Si} = 300$ nm for the silicon hybrid plasmonic waveguide, the calculated field distribution $E_y(x, y)$ for the quasi-TM fundamental mode is shown in Fig. 2(b). It can be seen that the field at the 50 nm-SiO_2 nano-layer is enhanced greatly. Because of the ultra-strong optical confinement and relatively low propagation loss, silicon hybrid nanoplasmonic waveguide has been attracting lots of attention and various hybrid nanoplasmonic waveguides with some modifications have been proposed in the following years [36–44].

Usually the metal absorption is not favorable for silicon photonics while the metal absorption loss can be possibly compensated by introducing some gain medium [37]. On the other hand, the light absorption of metal can be utilized to detect light power by utilizing the thermal-resistance effect of metal (heated by the incident optical power), as shown in Fig. 3 [45]. An electrical wheatstone bridge can be applied to accurately measure the resistance so that the resistance change of the metal strip is with very high sensitivity. Particularly, for silicon hybrid plasmonic waveguides, the nano-scale confinement of light enhances the thermal-resistance effect due to the metal absorption so that improved performances can be achieved in comparison with the traditional long-range surface plasmonic waveguides.

2.2 Silicon-plus photonics with III-V semiconductors

2.2.1 Adhesive bonding

Adhesive bonding is a classical technique to bring together two substrates of different materials [46]. Due to the soft and adhesive nature of the agent (usually polymers) applied between the two substrates, micro-structures (such as roughness) and unmatched material properties (such as thermal expansion coefficient) are largely compensated. As compared to other bonding techniques, adhesive bonding is more reliable and can provide a better yield. However, the drawback of this type of bonding comes from the bonding agent. Such an insulating polymer

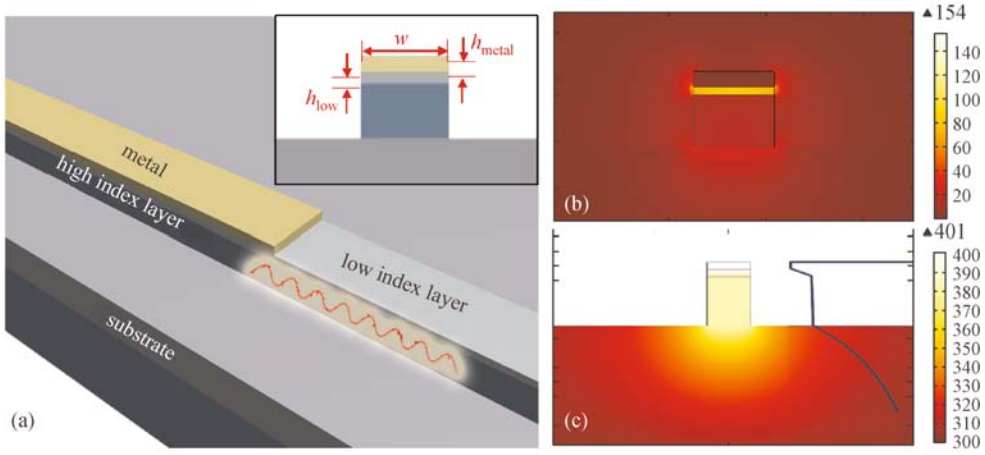

Fig. 3 Configuration of photodetector based on a silicon hybrid plasmonic waveguide (HPW). Inset shows the cross-section of silicon HPW [45]. (a) Schematic configuration; (b) optical mode field distribution; (c) temperature distribution due to the light absorption of metal

layer will prevent electrical contact. Although optical coupling, on the other hand, does not need a direct contact, the extra thickness presented by the polymer will also dramatically decrease the coupling strength of the photonic structures on the two substrates. By carefully choosing the polymer agent and optimizing the bonding procedure, a divinylsiloxane-bis-benzocyclobutene (DVS-BCB) layer of ~50 nm thickness has been successfully applied in bonding of IIIV epi-layers on top of a patterned silicon-on-insulator (SOI) wafer [47], as shown in Fig. 4(a). This enables the hybrid photonic integration of passive Si circuits with active functionalities provided by the IIIV materials using adhesive bonding technique.

Recently, we have developed a wavelength-multiplexed duplex transceiver module on a silicon chip using this type of bonding technology. A dual-functional hybrid-integrated active section based on the electro-absorption (EA) effect of an IIIV quantum-well structure is used for both modulation and detection [48], as shown in Fig. 4(b). Multilayer adiabatic tapers are used for light coupling between the passive access silicon waveguides and the active section [49]. Since the IIIV structure here is mostly straight, wet-etching technique is used to fabricate it. The undercut behavior of the wet-etching also facilitates to achieve an ultra-sharp tip-end of the taper, as shown in Fig. 4(c), which ensures low transmission losses of the whole structure. To expand the communication capacity, an arrayed-waveguide-grating (AWG) is also prepared in the module. There are six wavelength-channels with a spacing of 1.6 nm multiplexed or demultiplexed in the transmitter or receiver, respectively. On each channel, there is one hybrid-integrated active section. One fabricated chip is shown in Fig. 4(d). Since the modulation and detection both rely on the EA effect and eventually the same device structure, duplex link can therefore be realized. 30 Gb/s data transmission and receiving for each wavelength channel can be measured, as shown in Fig. 5. An aggregate data rate of 180 Gb/s is provided for the present transceiver module.

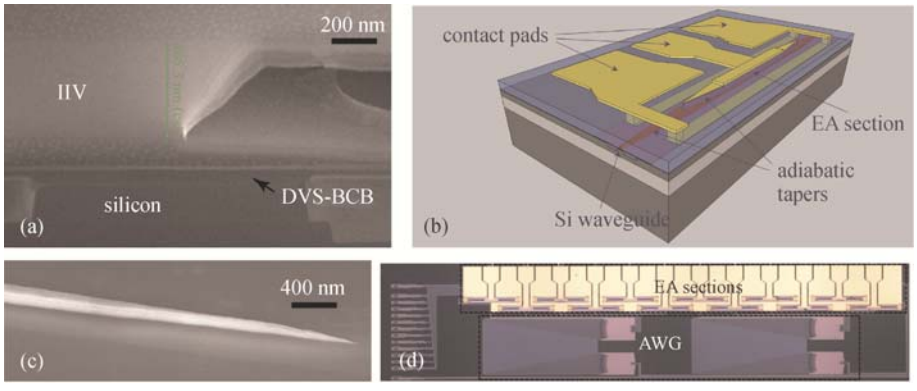

Fig. 4 (a) Cross section of a Si/IIIV hybrid integrated sample using the adhesive bonding technique; (b) schemetic structure of the present active section; (c) tip end of a fabricated adiabatic taper; (d) fabricated chip where two 6-channel transceivers are present. The total size is 3 mm × 0.65 mm [48]

2.2.2 Direct bonding

In addition to adhesive bonding, molecule bonding is a mainstream approach in the category of direct wafer bonding. Most of SOI wafers in Si photonics research and commercialization are made by this bonding technique. It relies on chemical reactions, namely polymerization reactions, to take place at the bonding interface to form strong covalent bond [50]. Equations (1) and (2) below show the polymerization reactions in widely used Si-to-Si, Si-to-SiO_2 or SiO_2-to-SiO_2 bonding, where two surfaces need to be passivated with a high density of polar hydroxyl groups (-OH) [51]. They are bridging bonds between the mating surfaces to enable spontaneous bonding at room temperature. A thermal anneal process is usually necessary to speed up the polymerization process to form strong Si-O-Si bonds and also drive the gas products (H_2O and H_2) out of the bonding interface [51]. Annealing process at more than 900°C is typical for the Si- or SiO_2-based bonding. To avoid excessive strain due to mismatch in thermal expansion coefficient between Si and IIIV materials, annealing temperature over 400°C is prohibited in IIIV-to-Si direct bonding where an element III or V in IIIV material will replace a Si element in Eq. (1). The same polymerization reactions still take place in Si-to-IIIV molecule bonding. But special processes like plasma surface treatment and forming outgassing channels in Si or SOI surface prior to bonding are necessarily developed to enable strong, high-yield InP-to-Si direct wafer bonding at a low annealing temperature of 300°C [52]. A smooth (< 1 nm RMS surface roughness), flat and clean surface is critical to the direct bonding quality, which can be readily achieved in modern semiconductor fabrication facilities. The interface oxide as a product of Eq. (2) is in the order of 10 nm, so proximity of Si and IIIV materials allows strong optical coupling between two parties.

$$\mathrm{Si-OH + Si-OH \rightarrow Si-O-Si + HOH(g)}, \quad (1)$$

$$\mathrm{Si + 2H_2O \rightarrow SiO_2 + 2O_2(g)}. \quad (2)$$

Recently developed hybrid IIIV-on-Si platform is a promising application of III-V-to-Si direct bonding technique [4]. Similar to the devices based on adhesive bonding technique discussed above, thin IIIV epitaxial layers are bonded onto SOI substrate to provide optical gain and interact with Si waveguide underneath [4]. Compact hybrid Si microring lasers fabricated on this platform are attractive candidates for low-power consumption transmitter/transceiver applications in data communication [53]. However, for almost all compact SOI-based photonic devices whose operation results in noticeable current flow in the semiconductor materials, such as carrier-injection mode Si microring modulators, hybrid or heterogeneous Si microring/micro-disk lasers, device heating can prevent devices from reaching high performance. The root cause is the thick (>800 nm typically) buried oxide (BOX) layer in the SOI wafers whose thermal conductivity is around 100× worse than that of the Si. So when current flows through the semiconductors, the finite serial resistance leads to significant joule heating which cannot be dissipated quickly due to compact footprint and thermal block by the BOX layer [54].

A recent novel design is to etch some trenches outside the device region but through the BOX layer to reach the Si substrate [55,56]. Then highly thermal conductive materials (e.g., Au or Gu) can fill up those trenches to act as thermal shunts, so the heat from the device can be "grounded" to the Si substrate quickly. Figure 6(a) shows the 3D schematic of such a hybrid Si microring laser with integrated thermal shunts. Both p-type and n-type electrodes (Fig. 6(b)) are connected with shunts surrounding the devices for efficient heat dissipation [56]. A drastic device performance improvement is demonstrated by a record-high 105°C continuous-wave (CW) operation in a 50 μm in diameter device in Fig. 6(c), 35°C higher than that of the identical device in the same chip but without thermal shunt [56]. Better thermal management also greatly enhances the dynamic performance. Direct modulation bandwidth was extended from 3 to 5.5 GHz at 25 mA injection current and a decent eye diagram at 12.5 Gbps with 7.9 dB extinction ratio was obtained under 35 mA injection current (Fig. 6(d)) [57]. Those performance improvement paves the way to deploy those lasers in a harsh environment like data centers where temperate can fluctuate between 30°C and 85°C.

2.2.3 Growth

While bonding technology based approaches provide a viable path toward a full on-chip optical link that incorporates lasers, amplifiers, modulators, photodiodes, etc., the circuit integration density and the mass-production

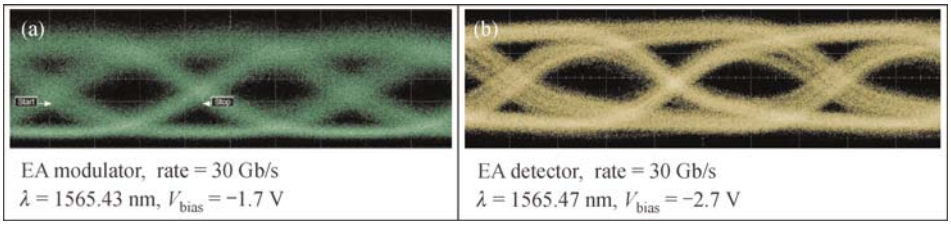

Fig. 5 Eye patterns of 2^7–1 on-return-to-zero pseudo random bit sequence for (a) modulation and (b) detection of one EA section [48]

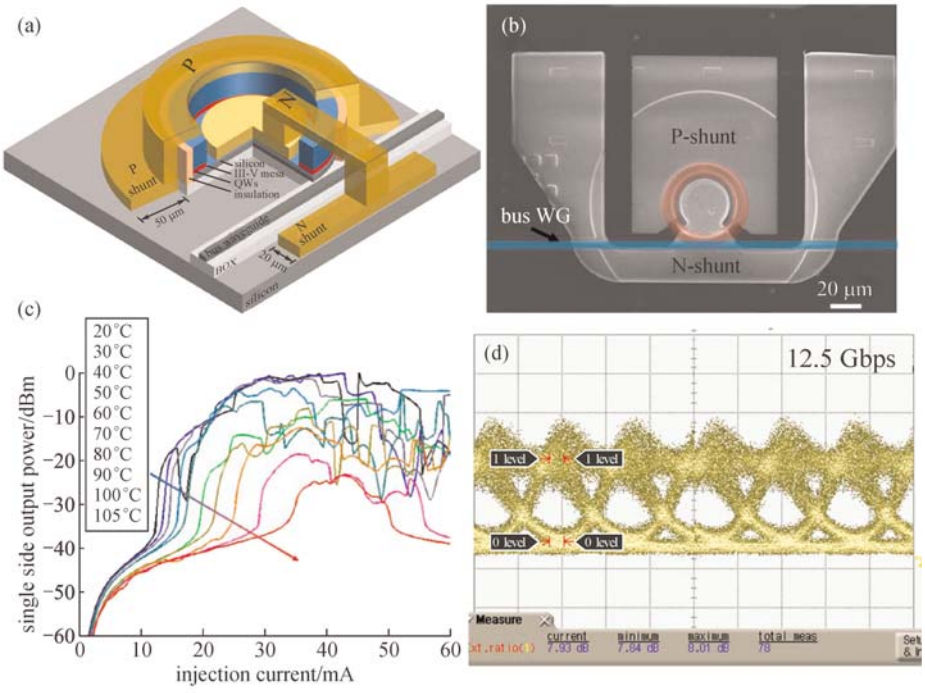

Fig. 6 (a) 3D schematic of a hybrid Si microring lasers with integrated thermal shunts; (b) top-view scanning electron microscope (SEM) image of such a device where ring laser and bus waveguide are highlighted in red and blue, respectively; (c) temperature-dependent LI characteristic and (d) measured eye diagram at 12.5 Gbps [56,57]

capacity are limited by the non-standard bonding process, which also increases the overall cost due to the inefficient use of III-V wafers. Therefore, for high volume, large integration density applications such as inter- or even intra-chip optical interconnects (promising for resolving the interconnect bottleneck), epitaxial growth of III-V semiconductors on silicon is more preferable. One could also fully enjoy the economies of scale offered by processing in advanced CMOS foundries.

Initiated more than three decades before, to grow high quality III-Vs on silicon, scientists have to overcome considerable hurdles. III-V semiconductors are intrinsically very different from silicon, in terms of lattice constant ($\varepsilon_{InP/Si}$ = 8.06%), thermal expansion coefficient and the interface polarity of the materials. Direct growth will results in high density of crystalline defects, including misfit and threading dislocations, twins, stacking faults and anti-phase boundaries, which considerably degrade the material quality for optoelectronics [58]. A few solutions have been proposed. By adding phosphorus, one may overcome the lattice-mismatch issue and grow high-quality GaP-related materials on (001)-Si substrates, and pulsed lasing has been achieved [59], while it is still challenging to move to the communication wavelength range. On the other hand, GaSb based room temperature laser has been integrated on silicon, regardless its highly mismatched lattice constant with silicon [60]. Besides the growth of planar layer of III-Vs on silicon, the direct integration of dimension-reduced materials on silicon, such as nanowires [61,62] and quantum dots [63,64], have also been extensively explored. Although it is relatively straightforward to grow high quality III-V nanowires on silicon, and room temperature lasing has been widely demonstrated, the precise control of laser position, the way of electrical injection, and the coupling of light with silicon waveguides are still very challenging. In addition, quantum dots (QDs) lasers on silicon have been realized with good thermal stability and high output power. However, a thick buffer layer is still required to accommodate the lattice mismatch, therefore the way of efficient light coupling into silicon waveguides requires considerable efforts in the future.

Localized growth of III-Vs on pre-patterned silicon wafer is another promising path toward large volume, highly dense integration of III-V optoelectronics on silicon. Thanks to the renewed interest of the electronics industry in using high-mobility compound semiconductors in next-generation CMOS [65], low defect-density growth of GaAs [19] and InP [20] using selective-area growth on pre-patterned (001)-Si has been demonstrated. By leveraging this technology, recently, it has been demonstrated that millimeter-long InP waveguide can be directly grown on silicon, with superior material quality (see the inset of Fig. 7(a)).

Based on this technology, optically pumped InP-on-Si distributed feedback laser (DFB) with robust single mode operation has been realized at room temperature (see the

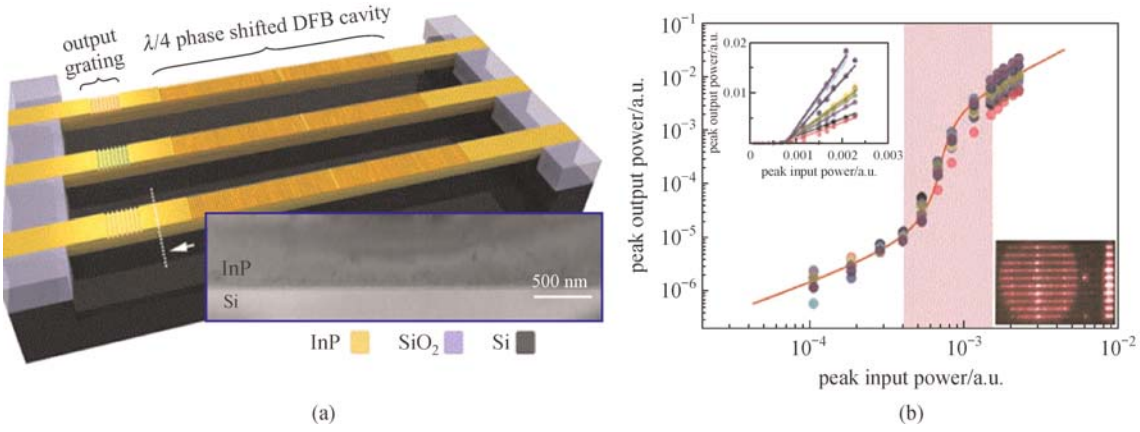

Fig. 7 (a) Schematics of an array of InP-on-Si distributed feedback laser (DFB) lasers. Inset: a transmission electron microscope (TEM) image of the grown InP-on-Si waveguide along the longitudinal direction; (b) light in-light out curves of an array of DFB lasers. Inset: photoluminescence image of an array of lasers under large area pump condition [21]

schematics of the laser in Fig. 7(a)) [21]. The well-understood in-plane laser configuration facilitates the co-integration of this DFB laser with silicon photonic and electronic circuits in the future, with the possibility of electrical injection. In addition, thanks to the technique of selective growth and the wafer-scale processing capability, it is straightforward to scale this technology to large volume and high integration density scenes. An array of DFB lasers with well-controlled emission wavelengths has been demonstrated. Relatively uniform lasing behavior of an array of 10 DFB lasers have also been presented (see Fig. 7(b)), illustrating the uniformity of the III–V material and devices and showing its promise for high capacity wavelength division multiplexing (WDM) applications.

While tremendous progress has been made on epitaxial growth of IIIV lasers on silicon, comprehensive reliability test on those monolithic lasers are still missing, mostly due to the fact that this research topic is still in its infancy. While threading dislocation can be mostly suppressed, the further evolution of other defects, such as twins, stacking faults and misfits at the IIIV/Si interface, under harsh operation conditions are still not fully studied. Tricks such as using defect filtering layers and QD based active layer can mitigate such problems. Recently, it is very encouraging to see the demonstration of electrically pumped IIIV quantum dot lasers on silicon with an extrapolated mean time to failure of over 100158 h.

2.3 Silicon-plus photonics with Ge

Ge is a type of group IV material and is likely to be compatible with silicon intrinsically. In recent years, great efforts had been made for the process of direct epitaxial growth of Ge on silicon and significant processes have been achieved. CMOS-compatible epitaxial growth of Ge has been realized with high quality. Therefore, Ge is considered as one of the most attractive candidates to realize active devices on silicon for optical fiber communications. For example, Ge-on-Si waveguide electro-absorption modulator with electro-optic bandwidth substantially beyond 50 GHz has demonstrated recently with a fully integrated silicon photonics platform on 200 mm silicon-on-insulator wafers [16]

It is also well known that Ge has absorption coefficient of ~10000 cm^{-1} at 1.31 μm and ~5000 cm^{-1} at 1.55 μm [66], and the absorption range can be even extended up to 1.6 μm by utilizing bandgap shrinkage related to tensile strain [6], which makes it useful for realizing photodetectors. With the Ge/Si platform, one can realize normal-incidence photodetectors for free-space or fiber-optic coupling [67], as well as waveguide-type photodetectors for on-chip integration [68]. Basically waveguide-type Ge/Si photodetectors are usually preferred because the carriers are collected in a direction perpendicular to the light propagation (absorption) direction [69]. In this way, the light absorption length is decoupled from the carrier collection path and consequently one can realize high-speed waveguide-type photodetectors with almost 100% quantum efficiency.

As Si is an ideal multiplication material because of the low $k < 0.1$ (defined as the ratio of the ionization rate of one carrier type to the other) [70], one should realize that the Ge-on-Si platform is very attractive for realizing avalanche photodiodes (APDs) with a separated absorption-charge-multiplication (SACM) structure. The first CMOS-compatible Ge/Si SACM APD was demonstrated by Kang et al. with a gain-bandwidth product (GBP) as high as 340 GHz [67]. Currently Ge/Si APDs have been very competitive in high-speed optical communication systems with higher GBPs and better sensitivity compared to traditional group III-V APDs [69]. Figure 8(a) shows waveguide-type Ge/Si APDs [71–73], which have two popular methods of coupling: evanescent coupling and butt-coupling, as shown in Figs. 8(b) and 8(c), respec-

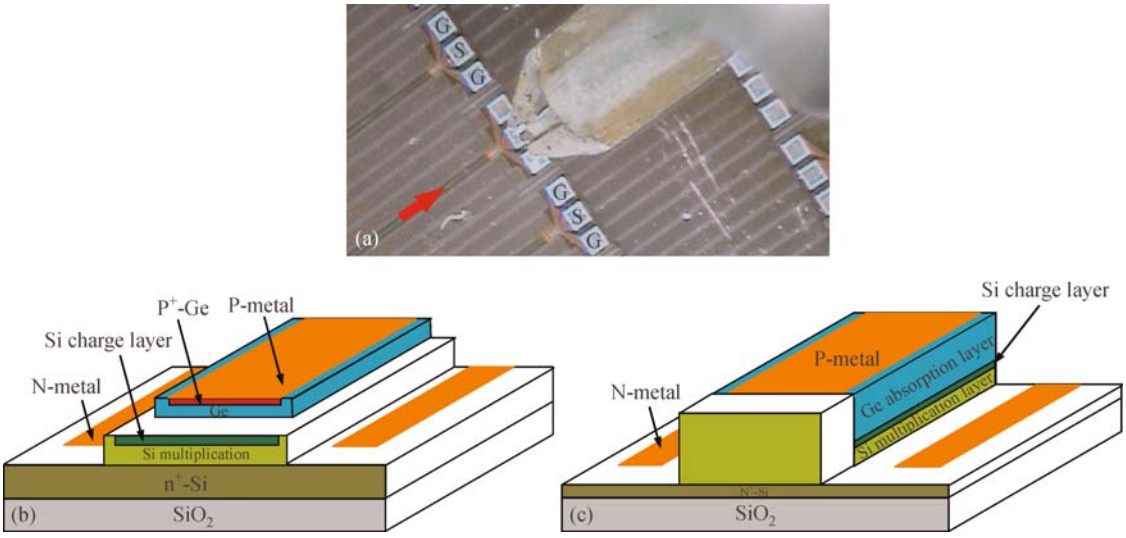

Fig. 8 (a) Microscope picture for waveguide-type Ge/Si SACM APDs; (b) an evanescently-coupled Ge/Si APD; (c) a butt-coupled Ge/Si APD [71]

tively. For the evanescently-coupled case, light guided in the silicon optical waveguide will be coupled evanescently to the Ge layer and be absorbed [74]. It is evident that butt-coupling is more efficient than the evanescent coupling because light directly enters the Ge absorption layer, and thus the photodiode length can be shortened to achieve higher bandwidth without compromising the responsivity. However the fabrication of the butt-coupled APD is complicated. The Ge/Si system is also an appealing candidate to realize high-efficiency fast photodiodes with large saturated output power for high-power applications, such as microwave photonics, because of the high thermal conductivities of Si and Ge, the durability and low cost of the substrate material [75]. High performance Ge/Si uni-traveling carrier (UTC) photodiodes have been realized recently [76].

As an indirect material, Ge has been used successfully for excellent photodetectors and modulators. It is also desired to overcome the limit of the indirect material and develop a Ge-on-silicon laser source, so that monolithic integration is enabled for realizing lab-on-a-chip as well as photonic network-on-chip. Note that the energy gap (0.8 eV) from the top of the valence band to the momentum-aligned Γ valley is close to the actual bandgap (0.66 eV). It is possible to compensate this small energy difference to form a laser gain medium by introducing heavy n-type doping as well as some tensile strain, as proposed in Ref. [19]. The first optically [20] and electrically pumped Ge-on-Si laser action in was reported by using Ge with a phosphorous doping level of $\sim 1 \times 10^{19}$ and 4×10^{19} cm^{-3}, respectively [77]. However, pump–probe measurements of similarly doped and strained material did not show evidence for net gain [22] and, in spite of numerous attempts, researchers have failed to substantiate the above results. Ge bandstructure can be also modified towards a direct-bandgap semiconductor when there is some tensile strain, which is usually enabled by introducing micromechanically stressed Ge membranes [9] or Si_3N_4 stressor layers [23]. A stressor-free technique was also presented to enable>5.7% [24] uniaxial tensile strain in Ge μ-bridges via selective wet under-etching of a prestressed layer [10]. An alternative technique to achieve a direct-bandgap material is to decrease the energy of the Γ-valley to below that of the L-valley, by incorporating sufficient Sn atoms into a Ge lattice to form a kind of GeSn alloys [78–80]. The major challenge is the low ($<1\%$) equilibrium solubility of Sn in Ge [81] and the large lattice mismatch of ~15% between them [80]. Partially and fully relaxed GeSn layers on Si [82] and on lattice-matched InGaAs ternary alloy [83] have been reported. Recently, Wirths et al. reported lasing in a direct-bandgap GeSn material and observed a threshold in emitted intensity and strong linewidth narrowing when $T \leqslant 90$ K [84]. This kind of direct-bandgap group IV materials may pave a way towards the CMOS-compatible monolithic integration on silicon.

2.4 Silicon-plus photonics with graphene

Graphene is well-known as a two-dimensional sheet of carbon atoms arrayed in a honeycomb structure, and has many unique optoelectronic properties [23], such as carrier mobility as high as 200000 $cm^2 \cdot V^{-1} \cdot s^{-1}$ at room temperature [85], broadband absorption of $\pi\alpha$ = ~2.3% per layer for vertically incident light, giant Kerr constants and other large optical nonlinearities [30]. These properties make graphene very attractive for many devices and applications, like photodetectors [8–10,86], modulators [7], and saturable absorbers [87].

To enhance the light-matter interactions, an interesting

approach is putting a graphene sheet on the top of an optical waveguide to form a kind of hybrid optical waveguide, so that the light-matter interaction is extended as long as the hybrid optical waveguide and on-chip graphene devices can be realized, as shown in Fig. 9. Particularly, this graphene-silicon platform is very useful for realizing active photonic integrated devices on silicon such as graphene electro-absorption modulators [7], waveguide-type graphene photodetectors [8–10], and some all-optical devices [87]. For example, in Ref. [28] a *local* and *non-local* optically induced transparency (OIT) effect in graphene-silicon hybrid photonic integrated circuits was demonstrated for the first time, which enables all-optical modulation over a broad wavelength range (see Figs. 10(a)–10(b)). This OIT effect is different from the saturated absorption effect in graphene reported previously [87]. For the saturated absorption effect, the graphene absorption was *locally* reduced at the position where the graphene sheet is illuminated by light, with an optical power density of up to 0.5~0.7 $\times$ 10^6 W/cm^2 from a high-power femto-second laser [87]. In contrast, for the OIT effect, a low-power continuous-wave laser is used and the power density to produce the OIT effect is extremely low, only ~2 W/cm^2, which can be achieved with carriers being generated in the silicon layer and injected into the graphene layer. This kind of OIT effect enables low power, all-optical, broadband control and sensing, modulation and switching *locally* and *non-locally*.

Graphene has very high intrinsic thermal conductivity and thus it is also potential to play an important role in the thermal managements for silicon photonics as heat spreaders, flexible heaters, etc. The graphene transparent flexible heat conductor is used to deliver heat from non-local metal heaters to a part of the nanophotonic integrated devices, as shown in Fig. 11(a)–11(b), which shows the thermally tuning silicon Mach-Zehnder interferometer (MZI) with a graphene heat conductor [88]. Because of the single-atom thickness and the transparency of graphene, the proposed graphene heat conductor can be utilized in almost any substrate or platform, such as silicon and silica. Furthermore, the excellent flexibility of graphene makes it available for complex surfaces with non-planar nanostructures.

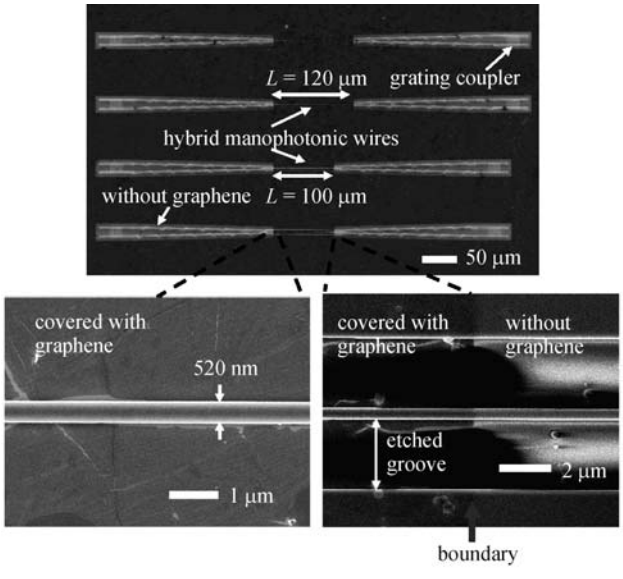

Fig. 9 SEM image of graphene-silicon hybrid nanophotonic wires [28]

Figure 12 shows an extremely small thermally tuning silicon micro-disk resonator (R = 5 μm) with a graphene heat conductor. The graphene heat conductor covers a part of the micro-disk to reduce excess loss, as shown in the inset of Fig. 12. From the measured dynamic spectral responses, it can be seen that the resonant wavelength of the micro-disk has a redshift of ~10 nm when the heating power varies from 0 to 38 mW. Therefore, the proposed transparent flexible graphene heat conductor is very convenient to achieve non-local heating for thermally tuning photonic integrated devices.

2.5 Silicon-plus photonics with polymer

Polymer materials can be synthesized as designed and thus have become a very important part for optoelectronic devices operating in visible light as well as near-infrared light. Furthermore, the fabrication processes for polymer photonic integrated circuits is very convenient and low-loss polymer optical waveguides have been developed [89]. As a result, polymer materials have been used widely for passive linear photonic integrated circuits. Particularly, for silicon-plus photonics, polymer materials also have some unique properties to be very useful [90].

First, polymer materials usually have a negative thermo-optical coefficient, which is comparable with that of silicon material. Therefore, it is promising to combine polymer materials with silicon photonic integrated circuits so that the significant temperature sensitivity of silicon photonic integrated circuits (PICs) can be compensated [91–93]. Second, one can design some polymer materials with high nonlinear optical coefficients, which helps realize high efficient nonlinear photonic devices on silicon. For example, when using electrical-optical polymer to fill in the nano-slot region of silicon nano-slot waveguides or metal nano-slot waveguides, one can have efficient electrical-optical modulation, which is useful for realizing high-speed optical modulation on silicon [94,95]. A 70 GHz all-plasmonic Mach-Zehnder modulator on silicon was demonstrated to enable high-speed optical communication at the microscale of ~10 μm. This dramatic size reduction helps achieve an ultra-low power consumption of 25 fJ/bit up to the highest speeds [96]. All-optical signal processing devices on silicon can also be realized by introducing some polymer materials with high nonlinear optical coefficients [11,12]. It is even possible to have

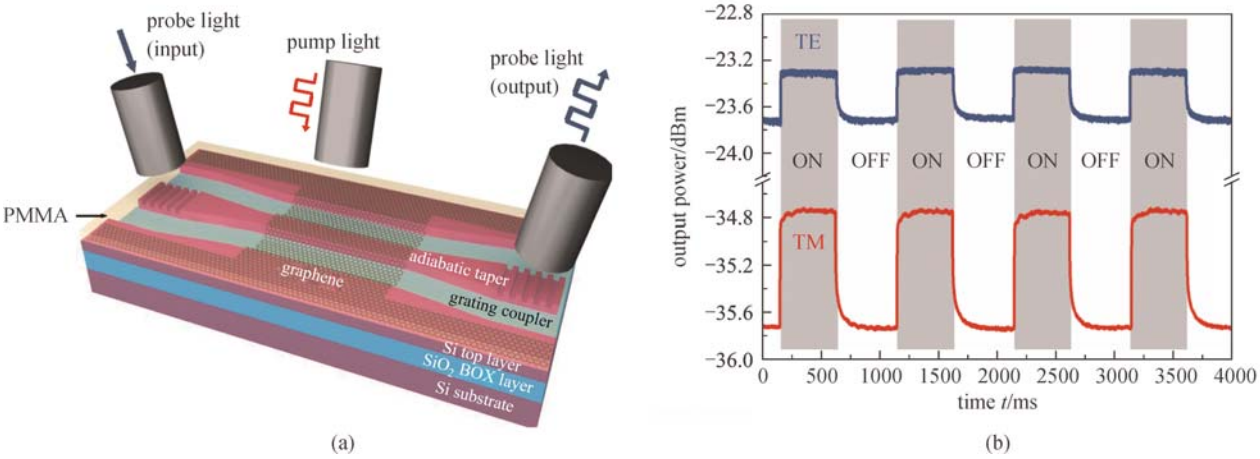

Fig. 10 (a) Three-dimensional schematic illustration of a graphene-silicon hybrid nanophotonic wire; (b) dynamic responses of the output power for TE- and TM- polarization modes with a modulated optical pump locally [28]

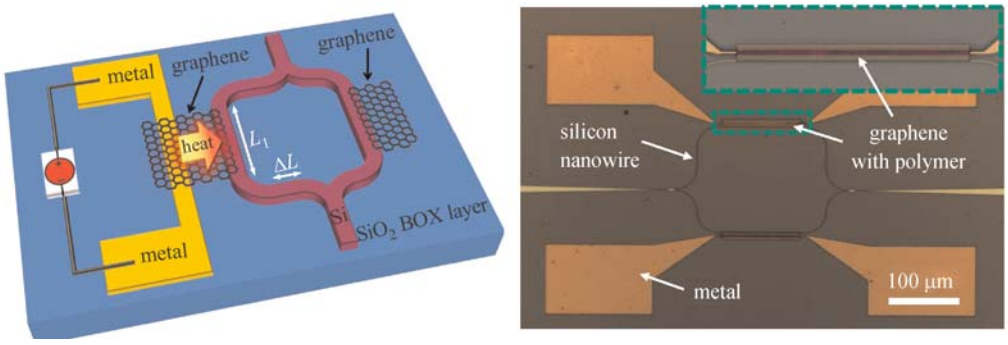

Fig. 11 A thermally tuning MZI with a non-local traditional metal heater and a graphene transparent flexible heat conductor [88]

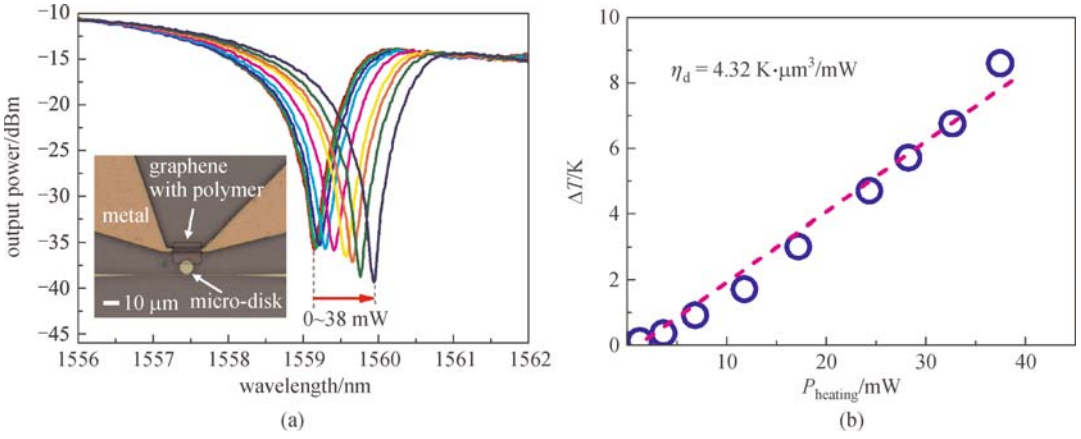

Fig. 12 A thermally tuning silicon micro-disk with a graphene transparent flexible heat conductor [88]

polymer materials with gain by doping some gain materials (like quantum dots, dye, etc.), which is very attractive to realize silicon-based optical amplifiers and even light emitters. In Ref. [97], Korn et al. demonstrated pulsed lasing at room temperature with peak output powers of up to 1.1 W at a wavelength of 1310 nm by combining standard SOI waveguides with dye-doped organic cladding materials. A challenge for silicon-plus photonics with

polymer is that polymer usually has rather low temperature stability, which might be an issue for the fabrication process and the practice use. People are trying to develop the polymer materials with improved temperature stability. Recently, a 64 GBd operation of a silicon-organic hybrid modulator at elevated temperature (~80°C) were demonstrated [98]. It is expected to have more exciting results on polymer materials for silicon photonics in the near future.

3 Conclusions

In this paper, we have given a discussion on silicon-plus photonics. Silicon-plus photonics makes silicon photonics more powerful by introducing other materials to complement the disadvantages of silicon. Currently, researchers have reported lots of materials, including metals, semiconductors, two-dimensional materials, polymer materials, etc., for working together with silicon photonics. All these materials help silicon realize various functionality elements, including lasers, photodetectors, modulators, amplifier, tunable/switchable devices, as well as the passive linear photonic devices. These achievements make it possible to realize large-scale photonic integrated circuits on silicon in the near future.

Acknowledgements This work was supported partially by the National Natural Science Foundation of China (Grant Nos. 61422510, 11374263 and 61431166001), the Doctoral Fund of Ministry of Education of China (No. 20120101110094), the Fundamental Research Funds for the Central Universities.

References

1. Hochberg M, Baehr-Jones T. Towards fabless silicon photonics. Nature Photonics, 2010, 4(8): 492–494
2. Asghari M, Krishnamoorthy A V. Silicon photonics: energy-efficient communication. Nature Photonics, 2011, 5(5): 268–270
3. Guan X, Wu H, Dai D. Silicon hybrid nanoplasmonics for ultra-dense photonic integration. Frontiers of Optoelectronics, 2014, 7(3): 300–319
4. Fang A W, Park H, Cohen O, Jones R, Paniccia M J, Bowers J E. Electrically pumped hybrid AlGaInAs-silicon evanescent laser. Optics Express, 2006, 14(20): 9203–9210
5. Park H, Kuo Y H, Fang A W, Jones R, Cohen O, Paniccia M J, Bowers J E. A hybrid AlGaInAs-silicon evanescent preamplifier and photodetector. Optics Express, 2007, 15(21): 13539–13546
6. Ishikawa Y, Wada K, Cannon D D, Liu J, Luan H C, Kimerling L C. Strain-induced band gap shrinkage in Ge grown on Si substrate. Applied Physics Letters, 2003, 82(13): 2044–2046
7. Liu M, Yin X, Ulin-Avila E, Geng B, Zentgraf T, Ju L, Wang F, Zhang X. A graphene-based broadband optical modulator. Nature, 2011, 474(7349): 64–67
8. Gan X, Shiue R, Gao Y, Meric I, Heinz T F, Shepard K, Hone J, Assefa S, Englund D. Chip-integrated ultrafast graphene photodetector with high responsivity. Nature Photonics, 2013, 7(11): 883–887
9. Pospischil A, Humer M, Furchi M M, Bachmann D, Guider R, Fromherz T, Mueller T. CMOS-compatible graphene photodetector covering all optical communication bands. Nature Photonics, 2013, 7(11): 892–896
10. Wang X, Cheng Z, Xu K, Tsang H K, Xu J. High-responsivity graphene/silicon-heterostructure waveguide photo-detectors. Nature Photonics, 2013, 7(11): 888–891
11. Koos C, Vorreau P, Vallaitis T, Dumon P, Bogaerts W, Baets R, Esembeson B, Biaggio I, Michinobu T, Diederich F, Freude W, Leuthold J. All-optical high-speed signal processing with silicon–organic hybrid slot waveguides. Nature Photonics, 2009, 3(4): 216–219
12. Melikyan A, Alloatti L, Muslija A, Hillerkuss D, Schindler P C, Li J, Palmer R, Korn D, Muehlbrandt S, Van Thourhout D, Chen B, Dinu R, Sommer M, Koos C, Kohl M, Freude W, Leuthold J. High-speed plasmonic phase modulators. Nature Photonics, 2014, 8(3): 229–233
13. Tien M C, Mizumoto T, Pintus P, Kromer H, Bowers J E. Silicon ring isolators with bonded nonreciprocal magneto-optic garnets. Optics Express, 2011, 19(12): 11740–11745
14. De Cort W, Beeckman J, Claes T, Neyts K, Baets R. Wide tuning of silicon-on-insulator ring resonators with a liquid crystal cladding. Optics Letters, 2011, 36(19): 3876–3878
15. Famà S, Colace L, Masini G, Assanto G, Luan H. High performance germanium-on-silicon detectors for optical communications. Applied Physics Letters, 2002, 81(4): 586–588
16. Srinivasan S A, Pantouvaki M, Gupta S, Chen H T, Verheyen P, Lepage G, Roelkens G, Saraswat K, Thourhout D V, Absil P, Campenhout J V. 56 Gb/s germanium waveguide electro-absorption modulator. Journal of Lightwave Technology, 2016, 34(2): 419–424
17. Chen L, Dong P, Lipson M. High performance germanium photodetectors integrated on submicron silicon waveguides by low temperature wafer bonding. Optics Express, 2008, 16(15): 11513–11518
18. Liu J, Camacho-Aguilera R, Bessette J T, Sun X, Wang X, Cai Y, Kimerling L C, Michel J. Ge-on-Si optoelectronics. Thin Solid Films, 2012, 520(8): 3354–3360
19. Guo W, Date L, Pena V, Bao X, Merckling C, Waldron N, Collaert N, Caymax M, Sanchez E, Vancoille E, Barla K, Thean A, Eyben P, Vandervorst W. Selective metal–organic chemical vapor deposition growth of high quality GaAs on Si(001). Applied Physics Letters, 2014, 105(6): 062101-1–062101-3
20. Merckling C, Waldron N, Jiang S, Guo W, Barla K, Heyns M, Collaert N, Thean A, Vandervorst W. Selective-area metal organic vapor-phase epitaxy of III–V on Si: what about defect density? ECS Transactions, 2014, 64(6): 513–521
21. Wang Z, Tian B, Pantouvaki M, Guo W, Absil P, Campenhout J V, Merckling C, Thourhout D V. Room-temperature InP distributed feedback laser array directly grown on silicon. Nature Photonics, 2015, 9: 837–842
22. Mueller T, Xia F, Avouris P. Graphene photodetectors for high-speed optical communications. Nature Photonics, 2010, 4(5): 297–301
23. Bonaccorso F, Sun Z, Hasan T, Ferrari A C. Graphene photonics

and optoelectronics. Nature Photonics, 2010, 4(9): 611–622
24. Bao Q, Loh K P. Graphene photonics, plasmonics, and broadband optoelectronic devices. ACS Nano, 2012, 6(5): 3677–3694
25. Hu Y, Pantouvaki M, Van Campenhout J, Brems S, Asselberghs I, Huyghebaert C, Absil P, Van Thourhout D. Broadband 10 Gb/s operation of graphene electro-absorption modulator on silicon. Laser & Photonics Reviews, 2016, 10(2): 307–316
26. Yu L, Xu Y, Shi Y, Dai D. Linear and nonlinear optical absorption of on-chip silicon-on-insulator nanowires with graphene. In: Proceedings of Asia Communications and Photonics Conference, 2012: AS1B. 3-1–AS1B. 3-3
27. Gu T, Petrone N, McMillan J F, van der Zande A, Yu M, Lo G Q, Kwong D L, Hone J, Wong C W. Regenerative oscillation and four-wave mixing in graphene optoelectronics. Nature Photonics, 2012, 6 (8): 554–559
28. Yu L, Zheng J, Xu Y, Dai D, He S. Local and nonlocal optically induced transparency effects in graphene-silicon hybrid nanophotonic integrated circuits. ACS Nano, 2014, 8(11): 11386–11393
29. Lee J M, Kim D J, Kim G H, Kwon O K, Kim K J, Kim G. Controlling temperature dependence of silicon waveguide using slot structure. Optics Express, 2008, 16(3): 1645–1652
30. Pollnau M. Rare-earth-ion-doped channel waveguide lasers on silicon. IEEE Journal of Selected Topics in Quantum Electronics, 2015, 21(1): 1602512-1–1602512-12
31. Chen S, Shi Y, He S, Dai D. Low-loss and broadband 2 × 2 silicon thermo-optic Mach-Zehnder switch with bent directional couplers. Optics Letters, 2016, 41(4): 836–839
32. Alam M Z, Meier J, Aitchison J S, Mojahedi M. Super mode propagation in low index medium. In: Proceedings of Quantum Electronics and Laser Science Conference, 2007, JThD112-1–JThD112-2
33. Oulton R F, Sorger V J, Genov D A, Pile D F P, Zhang X. A hybrid plasmonic waveguide for subwavelength confinement and long-range propagation. Nature Photonics, 2008, 2(8): 496–500
34. Fujii M, Leuthold J, Freude W. Dispersion relation and loss of subwavelength confined mode of metal-dielectric-gap optical waveguides. IEEE Photonics Technology Letters, 2009, 21(6): 362–364
35. Dai D, He S. A silicon-based hybrid plasmonic waveguide with a metal cap for a nano-scale light confinement. Optics Express, 2009, 17(19): 16646–16653
36. Dai D, He S. Low-loss hybrid plasmonic waveguide with double low-index nano-slots. Optics Express, 2010, 18(17): 17958–17966
37. Dai D, Shi Y, He S, Wosinski L, Thylen L. Gain enhancement in a hybrid plasmonic nano-waveguide with a low-index or high-index gain medium. Optics Express, 2011, 19(14): 12925–12936
38. Kwon M S. Metal-insulator-silicon-insulator-metal waveguides compatible with standard CMOS technology. Optics Express, 2011, 19(9): 8379–8393
39. Kim J T. CMOS-compatible hybrid plasmonic slot waveguide for on-chip photonic circuits. IEEE Photonics Technology Letters, 2011, 23(20): 1481–1483
40. Zhu S, Liow T Y, Lo G Q, Kwong D L. Silicon-based horizontal nanoplasmonic slot waveguides for on-chip integration. Optics Express, 2011, 19(9): 8888–8902
41. Bian Y, Zheng Z, Zhao X, Liu L, Su Y L, Liu J, Zhu J, Zhou T. Hybrid plasmonic waveguide incorporating an additional semiconductor stripe for enhanced optical confinement in the gap region. Journal of Optics, 2013, 15(3): 035503-1–035503-9
42. Amirhosseini A, Safian R. A hybrid plasmonic waveguide for the propagation of surface plasmon polariton at 1.55 μm on SOI substrate. IEEE Transactions on Nanotechnology, 2013, 12(6): 1031–1036
43. Alam M Z, Meier J, Aitchison J S, Mojahedi M. Propagation characteristics of hybrid modes supported by metal-low-high index waveguides and bends. Optics Express, 2010, 18(12): 12971–12979
44. Goykhman I, Desiatov B, Levy U. Experimental demonstration of locally oxidized hybrid silicon-plasmonic waveguide. Applied Physics Letters, 2010, 97(14): 141106-1–141106-3
45. Wu H, Guan X, Dai D. Ultracompact on-chip long-wave photodetector based on hybrid plasmonic waveguides. In: Proceedings of Piers, Session 1P4a SC2: Plasmonic Nanophotonics 1—Experiment, Measurement and Fabrication, 2014, 90
46. Niklaus F, Stemme G, Lu J Q, Gutmann R J. Adhesive wafer bonding. Journal of Applied Physics, 2006, 99(3): 031101-1–031101-28
47. Keyvaninia S, Muneeb M, Stanković S, Van Veldhoven P J, Van Thourhout D, Roelkens G. Ultra-thin DVS-BCB adhesive bonding of III-V wafers, dies and multiple dies to a patterned silicon-on-insulator substrate. Optical Materials Express, 2013, 3(1): 35–46
48. Fu X, Cheng J, Huang Q, Hu Y, Xie W, Tassaert M, Verbist J, Ma K, Zhang J, Chen K, Zhang C, Shi Y, Bauwelinck J, Roelkens G, Liu L, He S. 5 × 20 Gb/s heterogeneously integrated III-V on silicon electro-absorption modulator array with arrayed waveguide grating multiplexer. Optics Express, 2015, 23(14): 18686–18693
49. Huang Q, Cheng J, Liu L, Tang Y, He S. Ultracompact tapered coupler for the Si/III-V heterogeneous integration. Applied Optics, 2015, 54(14): 4327–4332
50. Gösele U, Bluhm Y, Kästner G, Kopperschmidt P, Kräuter G, Scholz R, Schumacher A, Senz S, Tong Q Y, Huang L J, Chao Y L, Lee T H. Fundamental issues in wafer bonding. Journal of Vacuum Science & Technology A, Vacuum, Surfaces, and Films, 1999, 17 (4): 1145–1152
51. Liang D, Roelkens G, Baets R, Bowers J E. Hybrid integrated platforms for silicon photonics. Materials (Basel), 2010, 3(3): 1782–1802
52. Liang D, Bowers J E. Highly efficient vertical outgassing channels for low-temperature InP-to-silicon direct wafer bonding on the silicon-on-insulator (SOI) substrate. Journal of Vacuum Science & Technology B Microelectronics and Nanometer Structures, 2008, 26 (4): 1560–1568
53. Liang D, Fiorentino M, Okumura T, Chang H H, Spencer D T, Kuo Y H, Fang A W, Dai D, Beausoleil R G, Bowers J E. Electrically-pumped compact hybrid silicon microring lasers for optical interconnects. Optics Express, 2009, 17(22): 20355–20364
54. Liang D, Fiorentino M, Srinivasan S, Todd S T, Kurczveil G, Bowers J E, Beausoleil R G. Optimization of hybrid silicon microring lasers. IEEE Photonics Journal, 2011, 3(3): 580–587
55. Liang D, Srinivasan S, Fiorentino M, Kurczveil G, Bowers J E, Beausoleil R G. Optimization of hybrid silicon microring lasers. IEEE Photonics Journal, 2011, 3(3): 580–587
56. Zhang C, Liang D, Kurczveil G, Bowers J E, Beausoleil R G.

Thermal management of hybrid silicon ring lasers for high temperature operation. IEEE Journal of Selected Topics in Quantum Electronics, 2015, 21(6): 1–7

57. Zhang C, Liang D, Li C, Kurczveil G, Bowers J E, Beausoleil R G. High-speed hybrid silicon microring lasers. In: Proceedings of 2015 IEEE 58th International Midwest Symposium on Circuits and Systems (MWSCAS), 2015, 1–4
58. Ayers J E. Heteroepitaxy of Semiconductors: Theory, Growth, and Characterization. New York: CRC Press, 2007
59. Hossain N, Sweeney S J, Rogowsky S, Ostendorf R, Wagner J, Liebich S, Zimprich M, Volz K, Kunert B, Stolz W. Reduced threshold current dilute nitride Ga(NAsP)/GaP quantum well lasers grown by MOVPE. Electronics Letters, 2011, 47(16): 931–933
60. Reboul J R, Cerutti L, Rodriguez J B, Grech P, Tournié E. Continuouswave operation above room temperature of GaSb-based laser diodes grown on Si. Applied Physics Letters, 2011, 99(12): 121113-1–121113-3
61. Chen R, Tran T T D, Ng K W, Ko W S, Chuang L C, Sedgwick F G, Chang-Hasnain C. Nanolasers grown on silicon. Nature Photonics, 2011, 5(3): 170–175
62. Wang Z, Tian B, Paladugu M, Pantouvaki M, Le Thomas N, Merckling C, Guo W, Dekoster J, Van Campenhout J, Absil P, Van Thourhout D. Polytypic InP nanolaser monolithically integrated on (001) silicon. Nano Letters, 2013, 13(11): 5063–5069
63. Chen S M, Tang M C, Wu J, Jiang Q, Dorogan V G, Benamara M, Mazur Y I, Salamo G J, Seeds A J, Liu H. 1.3 μm InAs/GaAs quantum-dot laser monolithically grown on Si substrates operating over 100°C. Electronics Letters, 2014, 50(20): 1467–1468
64. Wang T, Liu H, Lee A, Pozzi F, Seeds A. 1.3-μm InAs/GaAs quantum-dot lasers monolithically grown on Si substrates. Optics Express, 2011, 19(12): 11381–11386
65. del Alamo J A. Nanometre-scale electronics with III-V compound semiconductors. Nature, 2011, 479(7373): 317–323
66. Rouvière M, Halbwax M, Cercus J, Cassan E, Vivien L, Pascal D, Heitzmann M, Hartmann J, Laval S. Integration of germanium waveguide photodetectors for intrachip optical interconnects. Optical Engineering (Redondo Beach, Calif.), 2005, 44(7): 075402–075406
67. Kang Y, Liu H, Morse M, Paniccia M J, Zadka M, Litski S, Sarid G, Pauchard A, Kuo Y, Chen H, Sfar Zaoui W, Bowers J E, Beling A, McIntosh D C, Zheng X, Campbell J C. Monolithic Ge/Si avalanche photodiodes with 340 GHz gain-bandwidth product. Nature Photonics, 2009, 3(1): 59–63
68. Koester S J, Schaub J D, Dehlinger G, Chu J O. Germanium-on-SOI infrared detectors for integrated photonic applications. IEEE Journal of Selected Topics in Quantum Electronics, 2006, 12(6): 1489–1502
69. Michel J, Liu J, Kimerling L C. High performance Ge-on-Si photodetectors. Nature Photonics, 2010, 4(8): 527–534
70. Hawkins A R, Wu W, Abraham P, Streubel K, Bowers J E. High gain-bandwidth-product silicon heterointerface photodetector. Applied Physics Letters, 1997, 70(3): 303–305
71. Dai D, Piels M, Bowers J E. Monolithic germanium/silicon photodetectors with decoupled structures: resonant APDs and UTC photodiodes. IEEE Journal of Selected Topics in Quantum Electronics, 2014, 20(6): 43–56
72. Duan N, Liow T Y, Lim A E, Ding L, Lo G Q. 310 GHz gain-bandwidth product Ge/Si avalanche photodetector for 1550 nm light detection. Optics Express, 2012, 20(10): 11031–11036
73. Virot L, Vivien L, Fédéli J M, Bogumilowicz Y, Hartmann J M, Bœuf F, Crozat P, Marris-Morini D, Cassan E. High-performance waveguide-integrated germanium PIN photodiodes for optical communication applications. Photonics Research, 2013, 1(3): 140–147
74. Dai D, Chen H, Bowers J E, Kang Y, Morse M, Paniccia M J. Equivalent circuit model of a waveguide-type Ge/Si avalanche photodetector. Physica Status Solidi, 2010, 7(10): 2532–2535
75. Ramaswamy A, Piels M, Nunoya N, Yin T, Bowers J E. High power silicon-germanium photodiodes for microwave photonic applications. IEEE Transactions on Microwave Theory and Techniques, 2010, 58(11): 3336–3343
76. Piels M, Bowers J E. Si/Ge uni-traveling carrier photodetector. Optics Express, 2012, 20(7): 7488–7495
77. Liu J, Sun X, Camacho-Aguilera R, Kimerling L C, Michel J. Ge-on-Si laser operating at room temperature. Optics Letters, 2010, 35 (5): 679–681
78. Jenkins D W, Dow J D. Electronic properties of metastable Ge_xSn_{1-x} alloys. Physical Review B: Condensed Matter and Materials Physics, 1987, 36(15): 7994–8000
79. Low K L, Yang Y, Han G, Fan W, Yeo Y. Electronic band structure and effective mass parameters of $Ge_{1-x}Sn_x$ alloys. Journal of Applied Physics, 2012, 112(10): 103715-1–103715-9
80. Gupta S, Magyari-Köpe B, Nishi Y, Saraswat K C. Achieving direct band gap in germanium through integration of Sn alloying and external strain. Journal of Applied Physics, 2013, 113(7): 073707-1–073707-7
81. He G, Atwater H A. Interband transitions in Sn_xGe_{1-x} alloys. Physical Review Letters, 1997, 79(10): 1937–1940
82. Grzybowski G, Beeler R T, Jiang L, Smith D J, Kouvetakis J, Menéndez J. Next generation of $Ge_{1-y}Sn_y$ ($y = 0.01 - 0.09$) alloys grown on Si (100) via Ge_3H_8 and SnD_4: reaction kinetics and tunable emission. Applied Physics Letters, 2012, 101(7): 072105-1–072105-5
83. Chen R, Lin H, Huo Y, Hitzman C, Kamins T I, Harris J S. Increased photoluminescence of strain-reduced, high-Sn composition $Ge_{1-x}Sn_x$ alloys grown by molecular beam epitaxy. Applied Physics Letters, 2011, 99(18): 181125-1–181125-3
84. Wirths S, Geiger R, von den Driesch N, Mussler G, Stoica T, Mantl S, Ikonic Z, Luysberg M, Chiussi S, Hartmann J M, Sigg H, Faist J, Buca D, Grützmacher D. Lasing in direct-bandgap GeSn alloy grown on Si. Nature Photonics, 2015, 9(2): 88–92
85. Bolotin K I, Sikes K J, Jiang Z, Klima M, Fudenberg G, Hone J, Kim P, Stormer H L. Ultrahigh electron mobility in suspended graphene. Solid State Communications, 2008, 146(9-10): 351–355
86. Xia F, Mueller T, Lin Y M, Valdes-Garcia A, Avouris P. Ultrafast graphene photodetector. Nature Nanotechnology, 2009, 4(12): 839–843
87. Bao Q, Zhang H, Ni Z, Wang Y, Polavarapu L, Shen Z, Xu Q, Tang D, Loh K P. Monolayer graphene as a saturable absorber in a mode-locked laser. Nano Research, 2011, 4(3): 297–307
88. Yu L, Dai D, He S. Graphene-based transparent flexible heat conductor for thermally tuning nanophotonic integrated devices. Applied Physics Letters, 2014, 105(25): 251104-1–251104-5

89. Yang B, Yang L, Hu R, Sheng Z, Dai D, Liu Q, He S. Fabrication and characterization of small optical ridge waveguides based on SU-8 polymer. Journal of Lightwave Technology, 2009, 27(18): 4091–4096
90. Koos C, Leuthold J, Freude W, Kohl M, Dalton L R, Bogaerts W, Giesecke A L, Lauermann M, Melikyan A, Koeber S, Wolf S, Weimann C, Muehlbrandt S, Koehnle K, Pfeifle J, Palmer R, Alloatti L, Elder D L, Wahlbrink T, Bolten J.Silicon-organic hybrid (SOH) and plasmonic-organic hybrid (POH) integration. In: Proceedings of Optical Fiber Communication Conference and Exhition, 2015, Tu2A.1-1–Tu2A.1-3
91. Wang X, Xiao S, Zheng W, Wang F, Li Y, Hao Y, Jiang X, Wang M, Yang J. Athermal silicon arrayed waveguide grating with polymer-filled slot structure. Optics Communications, 2009, 282(14): 2841–2844
92. Lee J M, Kim D J, Ahn H, Park S H, Kim G. Temperature dependence of silicon nanophotonic ring resonator with a polymeric overlayer. Journal of Lightwave Technology, 2007, 25(8): 2236–2243
93. Teng J, Dumon P, Bogaerts W, Zhang H, Jian X, Han X, Zhao M, Morthier G, Baets R. Athermal Silicon-on-insulator ring resonators by overlaying a polymer cladding on narrowed waveguides. Optics Express, 2009, 17(17): 14627–14633
94. Lauermann M, Palmer R, Koeber S, Schindler P C, Korn D, Wahlbrink T, Bolten J, Waldow M, Elder D L, Dalton L R, Leuthold J, Freude W, Koos C. Low-power silicon-organic hybrid (SOH) modulators for advanced modulation formats. Optics Express, 2014, 22(24): 29927–29936
95. Koeber S, Palmer R, Lauermann M, Heni W, Elder D L, Korn D, Woessner M, Alloatti L, Koenig S, Schindler P, Yu H, Bogaerts W, Dalton L R, Freude W, Leuthold J, Koos C.Femtojoule electro-optic modulation using a silicon-organic hybrid device. Light: Science Application, 2015, 4(2): e255-1–e255-8
96. Haffner C, Heni W, Fedoryshyn Y, Niegemann J, Melikyan A, Elder D L, Baeuerle B, Salamin Y, Josten A, Koch U, Hoessbacher C, Ducry F, Juchli L, Emboras A, Hillerkuss D, Kohl M, Dalton L R, Hafner C, Leuthold J. All-plasmonic Mach–Zehnder modulator enabling optical high-speed communication at the microscale. Nature Photonics, 2015, 9(8): 525–528
97. Korn D, Lauermann M, Koeber S, Appel P, Alloatti L, Palmer R, Dumon P, Freude W, Leuthold J, Koos C. Lasing in silicon-organic hybrid waveguides. Nature communications, 2016, 7: 10864-1–10864-9
98. Lauermann M, Wolf S, Palmer R, Bielik A, Altenhain L, Lutz J, Schmid R, Wahlbrink T, Bolten J, Giesecke A L, Freude W, Koos C.64 GBd operation of a silicon-organic hybrid modulator at elevated temperature. In: Proceedings of Optical Fiber Communication Conference and Exhibition, 2015: Tu2A.5-1–Tu2A.5-3

Daoxin Dai received the B. Eng. degree from the Department of Optical Engineering, Zhejiang University (China), and the Ph.D. degree from Royal Institute of Technology (Sweden), in 2000 and 2005, respectively. He joined Zhejiang University as an assistant professor in 2005 and became an associate professor in 2007, a full professor in 2011. He visited the Chinese University of Hong Kong in 2005, and Inha University (Korea) in 2007. Dr. Dai worked at the University of California, Santa Barbara as a visiting scholar from the end of 2008 until 2011. His current research interests include silicon nanophotonics for optical interconnections and optical sensing. He has published about 130 refereed international journals papers (including 8 invited review papers), and holds 11 patents. Dr. Dai has been invited to give more than 30 invited talks and served as the program committee member or session chair for some top international conferences (including OFC 2013–2015). He is serving as the Associate Editor of the Journals of "*IEEE Photonics Technology Letters*", "*Optical and Quantum Electronics*" and "*Photonics Research*".